Dipole and electric quadrupole excitations in ^{40,48}Ca

T. Hartmann, J. Enders,* P. Mohr, K. Vogt, S. Volz, and A. Zilges
Institut für Kernphysik, Technische Universität Darmstadt, Schlossgartenstrasse 9, D-64289 Darmstadt, Germany
(Received 20 September 2001; published 5 February 2002)

Photon scattering experiments have been performed to investigate the structure of the two doubly magic nuclei ^{40,48}Ca. The method is highly selective to induce low-order multipole transitions, i.e., $E1$, $M1$, and $E2$ from the ground state. We determined the energies and spins of excited states and the absolute strengths of the γ decays in a model independent way. We find the summed electric dipole strengths below 10 MeV to exhaust the energy weighted sum rule by 0.023 and 0.27 %, respectively. The summed electric quadrupole strengths are $\Sigma B(E2)\uparrow = 332\ e^2\,\mathrm{fm}^4$ and $407\ e^2\,\mathrm{fm}^4$ for ^{40}Ca and ^{48}Ca, respectively. In order to explain the difference in the $E1$ strengths of the two isotopes several theoretical models are discussed.

DOI: 10.1103/PhysRevC.65.034301 PACS number(s): 21.10.Tg, 23.20.−g, 25.20.Dc, 27.40.+z

I. INTRODUCTION

Nuclear resonance fluorescence (NRF) or real photon scattering is perfectly suited to investigate low-order multipole excitations in atomic nuclei [1,2]. It is a method with very high sensitivity to detect $E1$, $M1$, and $E2$ transitions and provides a way of deriving the absolute strengths of these transitions model independently.

During the last few years, several experiments using NRF have been carried out to study the low-lying electric dipole strength distribution in various nuclei [3]. Much interest has been spent on the investigation of the so-called two-phonon state arising from the coupling of the 2_1^+ and 3_1^- collective states in the case of spherical nuclei as well as on the $J=1$ bandheads of octupole vibrational bands in the case of an nucleus with static quadrupole deformation. Such measurements have been performed mainly on nuclei in the $A>100$ mass region [3–5]. Especially the $N=82$ region was investigated in detail [6–9]. Also the $E1$ distribution of several tin isotopes has been studied systematically [10–12]. ^{88}Sr, ^{90}Zr, and ^{94}Mo representing the $N=50$ region have also been investigated [13–15]. In the light mass region experiments on the nuclei ^{48}Ti, ^{52}Cr, ^{56}Fe, and ^{58,60}Ni have been performed [16–20]. The preference of mainly heavy nuclei in many previous studies is due to the fact that here the two-phonon states can be found at very low energies of only a few MeV, whereas in light nuclei these states are situated at higher energies, which causes problems in NRF experiments. With the new NRF setup at the Darmstadt superconducting linear electron accelerator S-DALINAC we are now able to perform such high-precision (γ,γ') measurements up to energies of 10 MeV for the first time by avoiding the production of neutrons [21].

It would be very desirable to extend the systematic knowledge about the structure of $|2_1^+\otimes 3_1^-;1^-\rangle$ states to light nuclei to get information about whether this collective excitation mode persists in the lower mass region. In addition to that, it is very interesting to study ^{48}Ca because experimental information about lifetimes or transition strengths is rather sparse in this nucleus.

Another reason to study these isotopes are theoretical predictions concerning the electric dipole strength distribution in nuclei with neutron excess [22–25]. Several models predict a new excitation form—named the pygmy dipole resonance (PDR)—which is described in a simplified picture as a collective out-of-phase oscillation of a neutron-proton core against a skin of excess neutrons—at energies below the particle threshold. Experiments in very light nuclei such as ^{6}He [26], where it is suggested that an α-cluster is formed inside the nucleus (as proposed by Iachello also for heavy nuclei [27]), or ^{9,11}Be and ^{13}C [28,29] are prominent examples of nuclei exhibiting $E1$ strength at low excitation energies. A similar spatial structure as a neutron skin can be observed in ^{11}Be where a so-called halo structure of neutrons at a distance to the core is formed [30]. But especially in heavy nuclei such as ^{116,124}Sn [10], ^{138}Ba [31–33], ^{140}Ce [8], or ^{208}Pb [34] experiments point to the possible existence of a PDR. In the mass region $A\leqslant 40$ measurements have been done on ^{40}Ar [35,36], $^{16-18}$O [37,38], and $^{16-22}$O [39]. An inverse kinematic experiment using the Coulomb excitation method was also performed on ^{20}O [40]. In addition the nuclei ^{56}Fe and ^{58}Ni have been investigated with photon scattering experiments in view of their electric dipole response [18].

Obviously, within the simple picture of the oscillating neutron skin, the energy and strength of this excitation mode should strongly depend on the N/Z ratio. However, so far no systematic study about the influence of the N/Z ratio on this mode has been performed. To study the modification of the electric dipole distribution it would be very useful to compare measurements of isotopes with different neutron to proton ratios N/Z under the same experimental conditions. The Calcium isotopic chain suits very well to this task because five stable even-even isotopes exist with very different N/Z ratios (from ^{40}Ca with $N/Z=1.0$ to ^{48}Ca with $N/Z=1.4$). First results of the experiment have been published in our letter recently [41].

II. EXPERIMENTAL SETUP

The measurements have been performed at the improved NRF setup at the superconducting linear electron accelerator S-DALINAC at Darmstadt University of Technology. For the

*Present address: National Superconducting Cyclotron Laboratory, Michigan State University, East Lansing, MI 48824-1321.

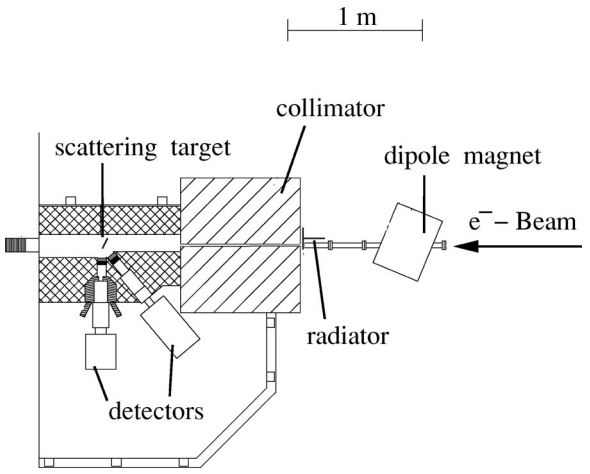

FIG. 1. The NRF setup at the S-DALINAC at Darmstadt University of Technology. The monoenergetic electron beam with energies up to 10 MeV and currents of typically 35 μA is stopped in a Cu radiator. The resulting γ radiation with a continuous energy distribution is collimated by a 95.5 cm long Cu collimator and strikes the scattering target. The decays of the excited nuclei to the ground state or other excited levels are detected by two HPGe detectors located at angles of 90° and 130° relative to the incoming photon beam.

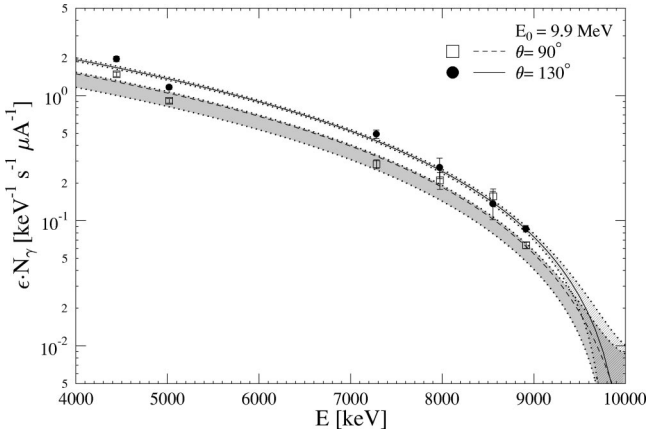

FIG. 2. The product of efficiency ϵ and absolute number of bremsstrahlung photons N_γ as a function of energy on a logarithmic scale. The data points represent six well known transitions in ^{11}B. The black circles show the data points for the detector at 90° and the squares for the one at 130°. The values were fitted with quadratic polynoms represented by the solid and dashed lines for the detectors at 130° and 90°, respectively. The shaded areas show the errors of the fits.

first time it was possible to perform photon scattering experiments up to excitation energies of 10 MeV without producing background resulting from (γ,n) and subsequent (n,γ) capture reactions in the surrounding and detector materials. Details about the setup can be found in Ref. [21].

A detailed scheme of the setup is shown in Fig. 1. The real photons are produced by fully stopping a monoenergetic electron beam in a 1.5 cm thick rotating, air cooled copper target. The uncertainty measuring the energy of the electron beam is about 150 keV. Between the bremsstrahlung source and the scattering probe a 95.5 cm thick copper collimator is installed. The scattering target was irradiated by the resulting γ beam. The scattered photons were detected by two HPGe (High Purity Germanium) semiconductor detectors—each with an efficiency of 100% relative to a $3''\times3''$ standard NaI detector—placed at angles of 90° and 130° with respect to the incoming beam. The distances of the detectors at 90° and 130° from the scattering target were 230 and 267 mm, respectively. The detector at 90° was surrounded by a BGO scintillation detector which works as an active Compton suppression shield. The detection system was completely shielded from the very high bremsstrahlung-background radiation by thick layers of lead. Between the scattering target and the detectors also 25 mm lead and 30 mm copper were installed to supress the lowest-energy photons scattered by the target.

The ^{48}Ca target—which was a loan from the GSI Darmstadt—consisted of 4706 mg CaO enriched to 82.7% in ^{48}Ca which means it contained 2977 mg ^{48}Ca. The ^{40}Ca target consisted of 4358 mg $^{\text{nat}}$CaO, containing 3014 mg ^{40}Ca. The energy and flux calibration was done with 783.3 mg $^{\text{nat}}$B. For the ^{40}Ca experiment we chose an endpoint energy of 9.9 MeV. ^{48}Ca was measured at three different endpoint energies of 5.5, 8.0, and 9.9 MeV. This was done to be able to distinguish between direct transitions to the ground state and inelastically scattered photons that means those that are emitted when the deexcitation occurs via another excited state. Some of the latter could be identified in ^{48}Ca because they disappear in measurements with lower endpoint energies, where the levels which are responsible for the feeding are no longer populated. The targets were irradiated for 114.5 h (^{48}Ca; 9.9 MeV), 41.5 h (^{48}Ca; 8.0 MeV), 45.5 h (^{48}Ca; 5.5 MeV), and 97.5 h (^{40}Ca).

III. DATA ANALYSIS

Here we give a brief introduction to the extraction of lifetimes and transition strengths from nuclear resonance fluorescence experiments. A detailed description can be found in Ref. [1,2].

From the measured integrals of the peak areas it is possible to derive the integrated cross section I^S of the ground state transitions

$$I^S = \frac{A_{i\to0}}{N_T \cdot N_\gamma(E_i) \cdot \epsilon(E_i) \cdot \Delta\Omega \cdot W_{eff}^{0\to i\to0}(\vartheta,\Delta\Omega)}. \quad (3.1)$$

The integral of the peak arising from the transition of the excited state i to the ground state 0 is given by $A_{i\to0}$. The number of target nuclei is denoted by N_T and N_γ is the absolute number of photons irradiating the target. The absolute detector efficiency is symbolized by ϵ. The solid angle covered by the detector is represented by $\Delta\Omega$. The angular distribution function is taken into account by W_{eff}.

To extract I^S it is necessary to know the product of absolute detector efficiency ϵ and integrated photon flux N_γ. This product can be extracted with the help of the boron calibration targets. $N_\gamma \cdot \epsilon$ is shown in Fig. 2 as a function of

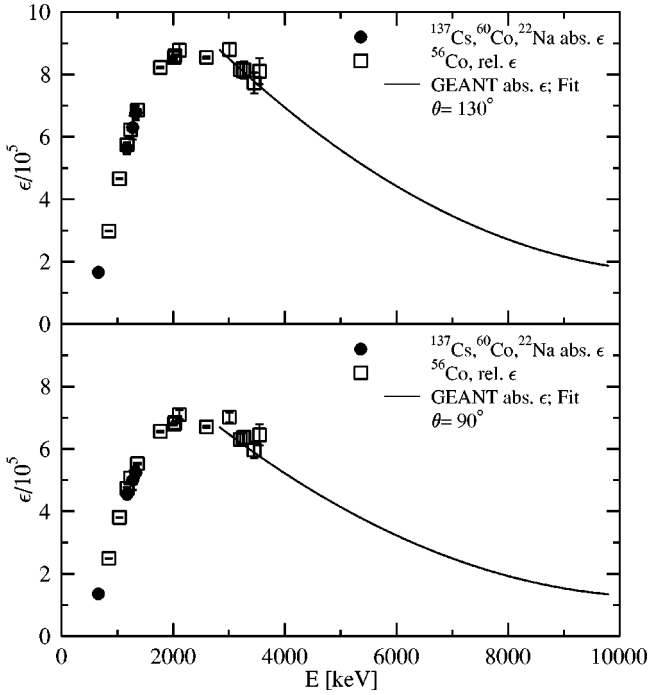

FIG. 3. Measured and simulated absolute efficiencies of the detectors. The filled circles show the measured values for the energies of transitions from the decay of ^{137}Cs, ^{60}Co, and ^{22}Na isotopes with known activites, the open squares show the relative values of transitions in the ^{56}Co decay scaled to fit the data at low energies and the lines show simulated absolute efficiencies.

energy. The data points represent the measured values for ground state transitions in ^{11}B and the lines are fitted to the data points.

For a deexcitation occuring via other excited states I^S can only be calculated if the detector efficiency itself is known and not only the product $N_\gamma \cdot \epsilon$ as discussed above. To achieve this we measured the efficiency at 20 energies up to 3550 keV with several radioactive sources such as ^{56,60}Co, ^{137}Cs, and ^{22}Na and simulated them for our geometry up to energies of 10 MeV with the Monte Carlo code GEANT [42] for 45 energies. The energies of the simulations were chosen to be the photon energies of the transitions in ^{11}B, ^{40}Ca, and ^{48}Ca detected in our experiment. The measured efficiencies and a fit through the simulated efficiencies is shown in Fig. 3. If the branching in other excited levels is known the total and partial level widths and lifetimes can be calculated. Because we used relatively thick targets, nonresonant and resonant selfabsorption in target and calibration material has to be considered. The nonresonant attenuation is handled by constructing the target as a sandwich target where the measured probe is enclosed between two discs of calibration material. The resonant absorption is considered by a correction factor $\eta(E)$ in the integral of the integrated cross section

$$I^S = \int dE\, \sigma(E) \cdot \eta(E). \tag{3.2}$$

The corrections to the data are of the order of 1 to 5 %. More details about the correction method can be found in Refs. [1,43].

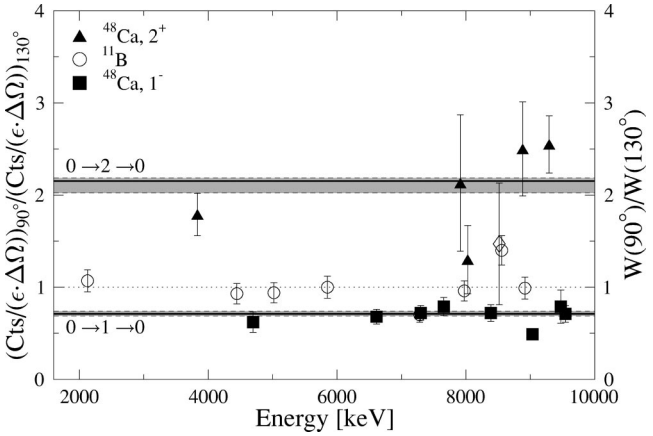

FIG. 4. The ratio of the measured, efficiency weighted radiation intensities at 90° and 130° (left axis) representing the angular distribution of the transitions compared to the ratios of the angular correlation functions for elastic scattering sequences (0→1→0) and (0→2→0) at 90° and 130° (right axis) represented by the horizontal lines with errors marked as grey areas arising from uncertainties in the detector positions. The triangles correspond to ground state transitions of levels with $J^\pi = 2^+$ and the squares to those of $J^\pi = 1^-$. The circles represent the excitations in ^{11}B, having almost uniform angular distributions. The diamond at the energy of 6421 keV is adopted in Ref. [44] as $J^\pi = 2^+$ state whereas we clearly identify it as a level with $J = 1$. For the level at 5628 keV we could not assign a spin unambiguously. Therefore we adopted the value given in Ref. [44].

To distinguish between dipole and quadrupole excitations the angular distribution of the scattered photons with respect to the incident beam is used.

The ratio of the efficiency corrected counts of the peak measured by the two detectors can be seen in Fig. 4 for excitations in ^{40}Ca and Fig. 5 for those in ^{48}Ca. We adopted parities from earlier experiments [44–48] if possible. Hitherto unobserved dipole transitions in ^{48}Ca were assumed to

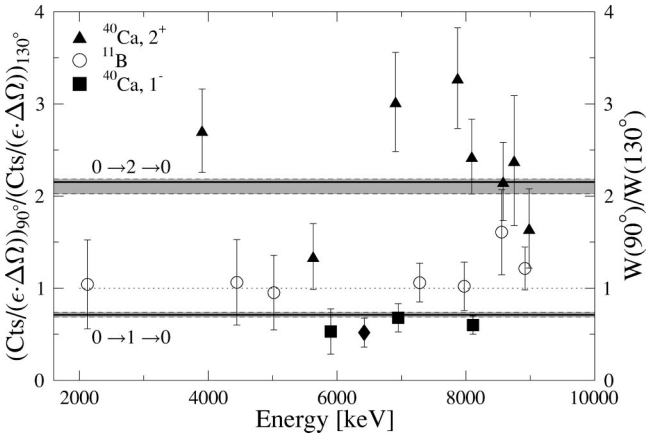

FIG. 5. Same caption as in Fig. 4. For the level at 8518 keV, which is symbolized by the diamond, no spin assignment was possible as for the level at 8027 keV. For the latter we adopted the value given in Ref. [44] while the other was observed in this experiment for the first time and therefore can only be restricted due to our experimental method to $J = 1,2$.

TABLE I. Ground state transitions in ^{40}Ca. Given are excitation energy E_x, spin and parity J^π, ground state transition width Γ_0, the corresponding transition strength $B(\sigma l)$, the lifetime τ, and the values for Γ_0 from Ref. [44]. Decay branches into low-lying known states have not been detected, and $\Gamma_0=\Gamma$ has been assumed. All parities are adopted from Ref. [44].

		This work			Adopted values in Ref. [44]
E_x [keV]	J^π [$\hbar$]	Γ_0 [meV]	$B(\sigma l)\uparrow$ [a]	τ [fs]	Γ_0 [meV]
3904.0(1)[b]	2^+	15.7(43)	107.6(292)	41.9(115)	19.4(11)
5249.6(3)	2^+[c]	4.6(5)	7.1(8)	143.1(156)	6.0(16)
5628.9(2)	2^+[d]	14.0(13)	15.4(14)	47.0(44)	12.4(28)
5902.5(2)	1^-	33.0(39)	0.46(5)	20.0(24)	36.6(61)
6421.2(9)	1[e]	27.1(70)	0.29(8)	24.3(63)	72.3(87)
6908.2(1)	2^+	220.8(358)	87.4(141)	3.0(5)	274.3(343)
6949.9(7)	1^-	489.3(710)	4.18(61)	1.3(2)	692.9(292)
7871.9(1)	2^+	176.1(321)	36.3(66)	3.7(7)	329.1(329)
8091.5(2)	2^+	166.2(160)	29.8(29)	4.0(4)	212.3(137)
8110.9(6)	1[f]	24.7(88)	0.13(5)	26.6(95)	17.3(77)
8578.7(2)	2^+	161.2(133)	21.6(18)	4.1(4)	134.3(164)
8749.4(2)	2^+	88.3(105)	10.7(13)	7.5(9)	94.0(269)
8982.5(5)	2^+	148.0(149)	15.8(16)	4.5(5)	73.1(163)

[a] $E1$ strength in $10^{-3}\,e^2\,\mathrm{fm}^2$, $E2$ strength in $e^2\,\mathrm{fm}^4$.
[b] Analyzed with the ^{48}Ca 5.5 MeV spectrum.
[c] Transition only observed in one detector. Therefore no spin deduced (adopted from Ref. [44]).
[d] Spin assignment ambiguous, adopted from Ref. [44].
[e] Spin and parity have been labeled as 2^+ in previous (γ,γ') experiment [53].
[f] Parity unknown.

be of electric nature because an earlier (e,e') experiment on this nucleus at backward angles did not detect any $M1$ strength with $B(M1)\uparrow > 0.15\ \mu_K^2$ below 10 MeV [49]. This corresponds to a limit of $B(E1)\uparrow \leqslant 1.66\times10^{-3}e^2\,\mathrm{fm}^2$. Therefore only three transitions could possibly have magnetic character as can be seen in Table I. Due to the small strengths their contribution to the total strengths is negligible.

With the simulated efficiencies and the measured product $N_\gamma\cdot\epsilon_{\mathrm{abs}}$ it is possible to calculate the absolute number of photons irradiating the scattering target at the discrete energies of the boron transitions. These data can be compared with a direct flux simulation up to 10 MeV. The latter one is less reliable than the simulation of the efficiencies especially at higher energies because interpolations between theoretical models are used to calculate the bremsstrahlung process at these energies. In contrast, the mass absorption coefficients for γ radiation needed to simulate the efficiencies are well known.

The extracted integrated photon flux can be seen in Fig. 6. The gray line shows the simulation which fails at high energies. This was considered with an energy dependent correction factor applied for energies above $0.8\times E_0$ of the following form:

$$F = 1 - 5\times10^{-4}\cdot\left(\frac{E-0.8E_0}{\mathrm{keV}}\right)^{3/4}. \tag{3.3}$$

This factor was chosen empirically to take into account the good agreement of the simulation up to energies below 80% of the endpoint energy and to take care of the fact that the photon flux has to become zero at the endpoint energy. Because the simulations showed the same discrepancies for different endpoint energies the starting point of the factor can be chosen to lie generally at 80% of the endpoint energy. For details of the correction procedure see Refs. [50,51].

The product of the functions for the number of photons and the detector efficiencies should lead to the same results

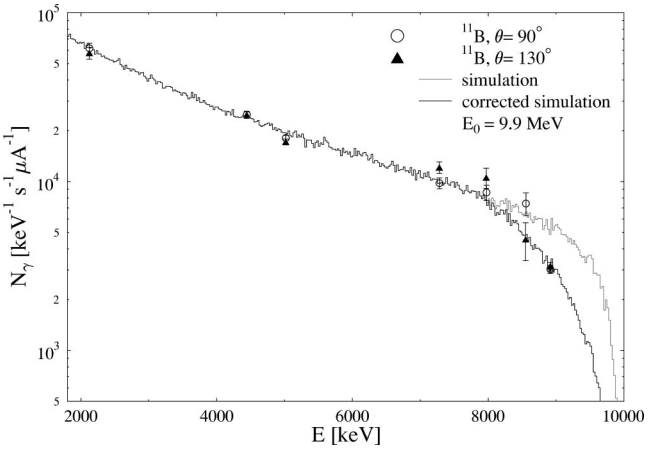

FIG. 6. The absolute number of photons as a function of energy. The triangles and circles show the ^{11}B data calculated from the measured peak areas and the simulated efficiencies. The grey line shows a first GEANT simulation of the absolute photon flux and the solid line is the corrected version of this simulation. The correction method is explained in detail in Refs. [50,51].

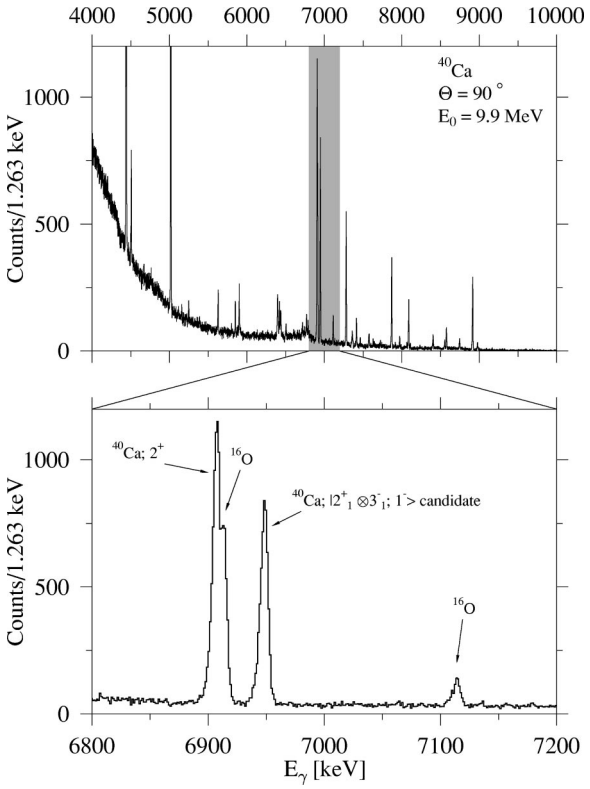

FIG. 7. Photon spectrum of ^{40}Ca (γ,γ') with an endpoint energy of 9.9 MeV measured at 90° with respect to the incoming beam. The levels at 5020 and 4444 keV exceeding the scale are transitions in ^{11}B. The lower part shows an enlarged view of the energy region between 6.8 and 7.2 MeV to demonstrate the energy resolution and the excellent peak-to-background ratio. Shown are singles spectra. No background was subtracted.

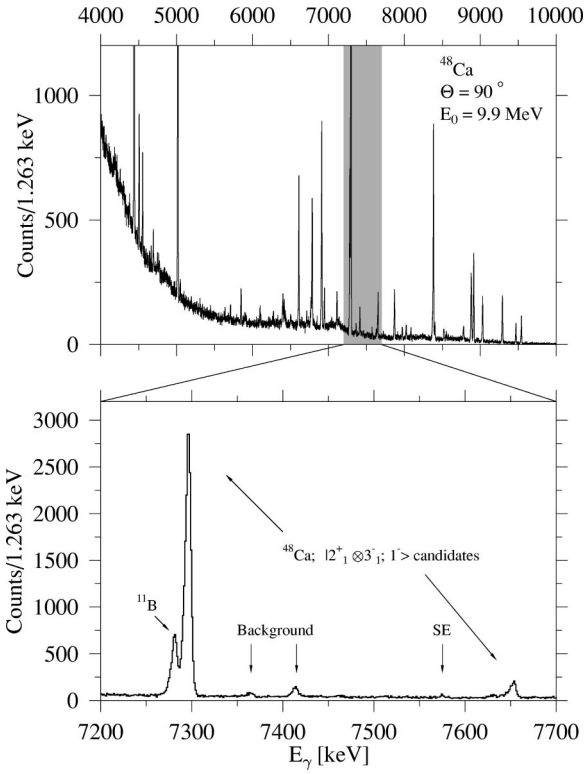

FIG. 8. Photon spectrum of ^{48}Ca (γ,γ') with an endpoint energy of 9.9 MeV taken at 90° with respect to the incoming beam. The peaks at 5020, 4444, and 7282 keV exceeding the scale are transitions in ^{11}B. The lower part shows an enlarged view of the energy region between 7.1 and 7.4 MeV to demonstrate the energy resolution and the excellent peak-to-background ratio.

in our analysis as the fit through the extracted product. Within the error bars this statement is true for all transitions.

IV. EXPERIMENTAL RESULTS AND DISCUSSION

The spectra of the measurements on the two calcium isotopes are shown in Figs. 7 and 8 for an endpoint energy of the bremsstrahlung of 9.9 MeV and an average electron current of 35 μA for 97.5 h and 114.5 h, respectively. This corresponds to a photon flux of about 10^6 photons/(keV s) at energies of about 7 MeV. The shaded areas in the upper parts are shown enlarged in the lower parts of the figures, to demonstrate the energy resolution and the high peak-to-background ratio.

All lines could be identified unambiguously (in their energetic position as known background, transitions in the target material, or systematic appearances as single- or double-escape peaks). The integrals of the peaks were extracted with the computer program VS [52]. The energy calibration was done with three well known γ transitions in ^{11}B at 2124.5, 5019.8, and 8916.3 keV.

The spectra—as shown in the enlarged parts—show the very good energy resolution of the detectors (2.3 at 1332 keV γ energy for both detectors and 6.4 and 6.8 keV at 8 MeV for the single crystal detector and segmented detector, respectively) and the very high peak to total ratio especially due to the use of an active anti-Compton BGO shield for the detector at 90°.

The measurement of ^{40}Ca enabled to separate the lines stemming from γ decays in the two different isotopes in the ^{48}Ca experiment which was nessessary because the ^{48}Ca target material contained a 15.8% contamination of ^{40}Ca. In addition we could check whether our results are consistent with an earlier experiment on ^{40}Ca by Moreh *et al.* [53] which mainly supplies the adopted values of Ref. [44]. The comparison of our results with Ref. [44] is given in Table I.

We assigned spin to the measured levels if the other possibility could be excluded by two standard deviations. In other cases we adopted the values from Ref. [44].

In the following we will discuss excited states in the two measured calcium isotopes in detail. The data are summarized in Tables I and II for ^{40}Ca and ^{48}Ca, respectively.

A. Excitations in ^{40}Ca

The level structure in ^{40}Ca is much better known than in ^{48}Ca. We found generally good agreement with data of earlier experiments [44].

The lowest 2^+ state in ^{40}Ca is the well established quadrupole vibrational state at 3904 keV. This level is strongly fed from other states, but we could deduce its lifetime from

TABLE II. Ground state transitions in ^{48}Ca. Given are excitation energy E_x, spin and parity J^π, branching ratio Γ_0/Γ, the ground state level width Γ_0, the corresponding transition strength $B(\sigma l)$, the lifetime τ, and the values for Γ_0 from Ref. [44]. Decay branches into low-lying known states have not been detected, and $\Gamma_0=\Gamma$ has been assumed. All parities are adopted from Ref. [44].

		This work				Adopted values in Ref. [44]
E_x [keV]	J^π [$\hbar$]	Γ_0/Γ	Γ_0 [eV]	$B(\sigma l)\uparrow$[a]	τ [fs]	Γ_0 [eV]
3831.5(2)	2^+	1.0	0.013(1)	96.8(105)	50.6(55)	0.0109(7)
4695.4(3)	1[b]	1.0	0.014(1)	0.38(3)	48.2(43)	
6612.2(1)	$1^{(-)}$	1.0	0.24(1)	2.4(2)	2.7(2)	
7298.5(2)	1[b, c]	1.0	2.24(13)	16.5(10)	0.29(2)	>0.0665
7655.7(2)	1[b, d]	1.0	0.21(1)	1.4(1)	2.7(1)	
7915.4(9)	2[b, d]	1.0	0.021(3)	4.2(7)	31.3(45)	
8027.6(4)	2^+[e]	1.0	0.040(4)	7.5(8)	16.5(17)	
8386.1(5)	1^-	0.91(8)	2.82(25)	12.5(8)	0.23(3)	
8517.9(8)[f]	1[b, d]	1.0	0.098(17)	0.45(8)	6.7(12)	
	2[b, d]	1.0	0.04(1)	5.6(14)	16.5(41)	
8883.5(5)	2^+	0.96(31)	1.16(1)	123.9(94)	0.6(2)	
9033.9(4)	1^-	0.98(40)	1.85(24)	7.0(9)	0.35(2)	
9295.3(2)	2[b, c]	1.0	1.95(12)	174.4(110)	0.34(2)	
9472.8(8)	1^-	1.0	1.81(15)	6.1(5)	0.36(3)	
9545.7(2)	1^-	1.0	3.27(21)	10.8(7)	0.20(1)	

[a] $E1$ strength in $10^{-3}\,e^2\,\mathrm{fm}^2$, $E2$ strength in $e^2\,\mathrm{fm}^4$.
[b] Parity unknown.
[c] Spin adopted in Ref. [44] differs from our value.
[d] Existing 3^- state with energy differing less than 4 keV adopted in Ref. [44].
[e] Spin assignment ambiguous, adopted from Ref. [44].
[f] No spin assignment possible.

the ^{48}Ca measurement at 5.5 MeV endpoint energy, where this state is still observed.

The ground state transitions of the levels at 5250 keV ($J^\pi=2^+$) and 8111 keV ($J=1$) were only observed in the detector at 90°. Therefore their spins could not be determined in this experiment and were adopted from Ref. [44]. This is due to the different peak-to-background ratios of the two detection systems because the segmented detector at 90° is shielded with an additional BGO-scintillation detector. The ratio of the peak-to-background ratios of the 90° and 130° detectors shows a linear behavior with a slope of approximately 0.719/MeV [54]. At 8 MeV the peak-to-background ratio of the detector at 90° is a factor of 5.7 higher than that of the detector at 130°.

A state which earns special attention is the one at 6421 keV. For this state we measured a value of $W(90°)/W(130°)=0.92\pm0.15$ that corresponds definitely to spin $J=1$. In contrast to that one other former NRF experiment performed by Moreh *et al.* [53] deduced the spin to be $J=2$. Assuming the level to have $J=2$, the width of this state were in agreement with the value of Moreh *et al.*

B. Excitations in ^{48}Ca

We found five $J=2$ states in the energy region up to 9.9 MeV. The lowest level at 3832 keV was analyzed in the spectrum at 5.5 MeV excitation energy to exclude feeding from higher-lying levels. A newly identified level is the one at 7915 keV, whereas the one at 8027 keV is quite well known.

Our spectra showed another ground state transition from a level at 8884 keV. The corresponding state is the origin of a inelastic transition to the 2_1^+ state which was observed at the energy of 5050 keV. The branching ratio to the ground state is $\Gamma_0/\Gamma=0.96$.

At 9295 keV the next state appears which has clear $J=2$ character. Near in energy literature gives a 9292 keV state with $J^\pi=1^-$. The nuclear spin was deduced from a DWBA analysis of momentum transfer reactions as (p,p') and (α,α') data. Natural parity was assigned because of the presence of the peak in (α,α') spectra.

Eight $J=1$ states below 9.9 MeV were found in the spectrum. The multipole order for the deexcitation from a level at 8518 keV cannot be deduced clearly. Table II therefore contains the results for the two possible angular distributions.

For the levels at 6612 keV, 9473 keV, and 9546 keV, the lifetime could be extracted for the first time. In addition we extracted their spin to be $J=1$. We observe a ground state transition at the energy of 7298 keV with spin $J=1$ which is proposed in literature to have $J=2$.

These three states have counterparts in literature that deviate only a few keV in excitation energy and have equal spin assignment. The states at 4694 keV and 7656 keV have not been observed before. Their lifetimes and spins could be

TABLE III. Photon energies from inelastic transitions in ^{48}Ca. The final level in all cases is the one at 3831.5 keV with $J^{\pi}=2^{+}$. For all transitions the mixing parameter δ was assumed to be zero.

E_γ [keV]	E_i [keV]	$\frac{\Gamma_i}{\Gamma}$ [meV]	Γ_i
4554.2(92)	8386.1(5)	0.090(3)	261(18)
5050.6(9)	8883.5(5)	0.040(10)	48(13)
5200.9(15)	9033.9(4)	0.022(9)	43(18)

extracted from our data. Two other states with $J=1$ were measured at 8386 keV and 9034 keV and have been observed in proton scattering experiments before. Both levels deexcite not only to the ground state but also to the first excited 2^{+} state at 3832 keV. The energies of the inelastic transitions are 4554 keV and 5201 keV with a branching ratio of $\Gamma_0/\Gamma=0.91$ and 0.98, respectively. All inelastic transitions are listed in Table III.

C. E1 strength distribution

1. Comparison of ^{40}Ca and ^{48}Ca

The $B(E1)\uparrow$ strength distributions of the two calcium isotopes are shown in Fig. 9. In the upper part the data collected previously in Ref. [44] are included for comparison. The lower part shows our data on ^{48}Ca where no comparison was possible because almost no strength information existed before. The dotted lines represent the sensitivity limit of our measurements with the specific setup and geometry.

In the lines 1–4 of Table IV the measured summed $B(E1)\uparrow$ strengths are listed. Below 10 MeV the sum amounts to $55.7(41)\times10^{-3}\,e^2\,\mathrm{fm}^2$ in ^{48}Ca which is one order of magnitude higher than in ^{40}Ca $[5.1(8)\times10^{-3}\,e^2\,\mathrm{fm}^2]$.

The summed energy-weighted dipole strength below 10 MeV is (467.0 ± 35.0) keV e^2 fm^2 and (34.7 ± 5.5) keV e^2 fm^2

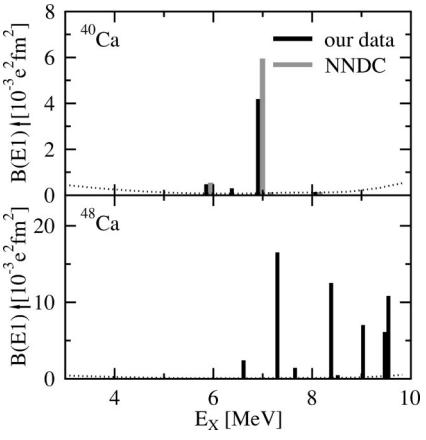

FIG. 9. Electric dipole strength distributions for ^{40}Ca (upper part) and ^{48}Ca (lower part). The strengths of ^{40}Ca are compared to NNDC data [44] which are mainly based on the results of Moreh *et al.* [53]. Please note the different scales. The dotted line shows the sensitivity limit of the measurements.

TABLE IV. Summed electric dipole and quadrupole strengths in ^{40}Ca and ^{48}Ca between 5 and 10 MeV.

		^{40}Ca	^{48}Ca
$\Sigma B(E1)\uparrow$	$[10^{-3}\,e^2\,\mathrm{fm}^2]$	5.1(8)	55.7(41)
$\Sigma B(E1)$	[m W.u.]	6.8(11)	21.8(16)
$\Sigma EB(E1)\uparrow$	$[\mathrm{keV}\,e^2\,\mathrm{fm}^2]$	34.7(55)	467.0(350)
$\Sigma EB(E1)\uparrow$	[%EWSR]	0.023(4)	0.27(2)
$\Sigma B(E2)\uparrow$	$[e^2\,\mathrm{fm}^4]$	332(60)	407(32)
$\Sigma B(E2)$	[W.u.]	8.2(15)	7.9(6)
$\Sigma B(E2)$	[%EWSR]	20.3(31)	34.0(33)

for ^{48}Ca and ^{40}Ca, respectively. Since the classical energy weighted sum rule (EWSR) for electric dipole strength [55] is given by

$$S(E1)_{\mathrm{class}}=\frac{9}{4\pi}\,\frac{\hbar^2e^2}{2M}\,\frac{NZ}{A}=14.8\,\frac{NZ}{A}\ \mathrm{MeV}\,e^2\,\mathrm{fm}^2$$

we find for the $E1$ strength up to 10 MeV in ^{40}Ca an exhaustion of 0.023(4)% of the EWSR, while in ^{48}Ca this value is 0.27(2)%.

Finally, another thing to look at is the electric polarizability of the two isotopes. It is given by $\Sigma_i B(E1)_i/E_i$ and presents information about how easy the center of charge can be separated from the center of mass in the nucleus. The values for the two calcium isotopes are $0.74(12)\times10^{-3}\,e^2\,\mathrm{fm}^2/\mathrm{MeV}$ and $6.93(52)\times10^{-3}\,e^2\,\mathrm{fm}^2/\mathrm{MeV}$ for ^{40}Ca and ^{48}Ca, respectively. That means that in the energy region between 5 and 10 MeV it is approximately 7 times easier to induce an electric dipole moment in ^{48}Ca due to the separation of the center of charge from the center of mass than it is the case in ^{40}Ca.

One can see that there exists a dramatic difference in the $B(E1)\uparrow$ strength distributions of the two isotopes. From the strength distribution of ^{48}Ca no clear resonance structure can be assigned. Unfortunately we are not able to continue our (γ,γ') measurement to higher excitation energies.

2. Comparison with previous experiments

Another experimental comparison of the electric dipole strength distributions of the two calcium isotopes was performed recently [56]. Here, ^{40}Ca and ^{48}Ca were studied in ^{40,48}Ca(^{86}Kr,^{86}Kr$'$)^{40,48}Ca heavy ion scattering reactions. The results for the summed $E1$ strength below 10 MeV from this study is 7.5(18)% and 6.7(33)% for the EWSR in ^{40}Ca and ^{48}Ca, respectively. This is in sharp contrast to our results.

Heavy-ion scattering, however, does not allow the electromagnetic transition strength to be determined model independently. Our experiments are model independent, exhibit high resolution resolving single excitations and are characterized by a low detection limit. Therefore our results exclude those from Ref. [56] clearly.

3. Excitations above the particle threshold

Comparing the two calcium isotopes, one possible explanation for missing $E1$ strength in ^{40}Ca may be the different particle emission thresholds. The energy required to emit a neutron is uncritical in our case for both isotopes ($S_n = 15.641$ MeV for ^{40}Ca and 9.946 MeV for ^{48}Ca). The energy for proton emission is much lower in ^{40}Ca than in ^{48}Ca ($S_p = 8.329$ MeV for ^{40}Ca and 15.807 MeV for ^{48}Ca) and below the endpoint energy of our bremsstrahlung. States above 8.4 MeV in ^{40}Ca can thus in principle decay also via proton emission which would not be detected in our experiments. However, such a decay channel would contribute to the ground state transition strength because the photon scattering cross section is given by $\sigma_0 \sim \Gamma_0^2/\Gamma$, where Γ is the total width including also particle channels. With the simplified assumption that ^{40}Ca is a pure system $^{39}\mathrm{K}+p$ one can derive an upper limit for this effect. The proton decay widths can be estimated with the help of the Wigner limit which takes into account the hindrance effect caused by the Coulomb barrier and is given by

$$\Gamma(E) = 2|\vec{k}|R_N\left(\frac{3\hbar^2}{2\mu R_N^2}\right)P_l(E,R_N) \tag{4.1}$$

with $\vec{k}$ symbolizing the propagation vector of the wave function, R_N being the nuclear radius, P_l the penetration factor of the Coulomb wave function, and μ the reduced mass. An approximation of the width of the proton channel (assuming a nuclear radius for ^{40}Ca of 4 fm) shows that one gets significant values of the order of eV from energies of 0.6 MeV above the proton threshold (8.4 MeV). Therefore below 9 MeV no significant proton decay width exists, and our results do not need to undergo any correction. To get information about the possible additional electric dipole strength above 9 MeV one has to consider states with $J^\pi = 1^-$ which have been seen in the reaction $^{39}\mathrm{K}(p,\gamma)^{40}$Ca [57]. In Table V all states with $J=1$ are listed together with the values of $S(p,\gamma)$ given by

$$S(p,\gamma) = (2J+1)\frac{\Gamma_p \cdot \Gamma_\gamma}{\Gamma} \tag{4.2}$$

with

$$\Gamma = \Gamma_p + \Gamma_\gamma$$

and

$$\Gamma_p \gg \Gamma_\gamma$$

follows

$$\frac{S(p,\gamma)}{(2J+1)} = \Gamma_\gamma. \tag{4.3}$$

The parities of the states are unknown in almost all cases. We are looking for an upper limit of the proton decay channel, so we assume that all $J=1$ states between 9 and 10 MeV have negative parity.

TABLE V. Upper limit of the γ level width of electric dipole states in ^{40}Ca above 9 MeV. The values for Γ_0 were calculated under the assumption of ^{40}Ca being a pure $^{39}\mathrm{K}+p$ system. Where the branching ratio of the photon channel is unknown—as in most cases—we assumed $\Gamma_0/\Gamma_\gamma = 1$. This makes an upper limit of the summed level width above 9 MeV of 5.1(19) eV. The branching ratios were taken from Ref. [57]. The $S(p,\gamma)$ values are adopted from Ref. [46].

E_x [keV]	$S(p,\gamma)$ [eV]	Γ_0/Γ	Γ_0 [eV]	$B(E1)\uparrow$ [$10^{-3}\,e^2\,\mathrm{fm}^2$]
9226.7	0.28(11)	0.118(10)	$1.1(4)\cdot 10^{-2}$	$4.0(15)\cdot 10^{-2}$
9227.4				
9429.1	2.8(11)	0	0	0
9432.5				
9537.9	0.24(10)		$\leqslant$0.08(3)	$\leqslant$0.26(10)
9604.6	5(2)		$\leqslant$1.67(67)	$\leqslant$5.4(22)
9655.6	0.22(9)		$\leqslant$0.07(3)	$\leqslant$0.22(10)
9785.3	1.0(4)		$\leqslant$0.33(13)	$\leqslant$1.0(4)
9802.2	0.37(15)		$\leqslant$0.12(5)	$\leqslant$0.37(15)
9811.1	0.27(11)		$\leqslant$0.09(4)	$\leqslant$0.27(12)
9829.5	0.8(3)		$\leqslant$0.27(10)	$\leqslant$0.82(30)
9854.5	1.1(4)		$\leqslant$0.37(13)	$\leqslant$1.11(39)
9865.2	6(2)	0.73	1.46(49)	4.36(146)
9869.3	3.1(12)	0.45	0.47(18)	1.4(5)
9921.4	0.43(17)		$\leqslant$0.14(6)	$\leqslant$0.41(18)
Σ			$\leqslant$5.08(191)	$\leqslant$19.6(52)

The values of $S(p,\gamma)$ are proportional to the total decay width Γ_γ of the level which is the sum of all partial decay widths. We are interested in the electromagnetic excitation strength from the ground state of the nucleus which is only related to the ground state decay width Γ_0. Therefore we had to take into account the branching of the excited states. Since the branching of 9 of the 13 states with spin $J=1$ is unknown, we assumed $\Gamma_0/\Gamma_\gamma = 1$ in those cases—which again is the most limiting hypothesis. The adopted values for $S(p,\gamma)$ together with the deduced values for $\Gamma_{i\to 0}$ and $B(E1)\uparrow$ are listed in Table V. As can be seen the upper limit of the summed ground state decay width of states with $J=1$ in ^{40}Ca above 9 MeV is $\Gamma_{i\to 0}^{\mathrm{est}} = 5.1(19)$ eV. Together with our measured values below 9 MeV [(0.57±0.09) eV, see Table IV] this gives an upper limit of $\Gamma_{i\to 0} = 5.7(20)$ eV below 10 MeV. In summary, the ratio of the summed $B(E1)$ strengths in ^{48}Ca and ^{40}Ca based on an upper limit for the proton decay branch in ^{40}Ca is still greater than 2.8, i.e., there is a significant difference in the $E1$ strength between the two isotopes. Please note that this is the most conservative estimate. Because of the fact that the doubly magic nucleus ^{40}Ca is not at all the pure system $^{39}\mathrm{K}+p$ and branchings to other excited states are very likely a much higher ratio seems to be more realistic.

4. Possible sources of E1 strength

To explain the difference in the electric dipole strength distribution is a challenging and interesting task. One ques-

tion is if the $E1$ strength is collective or if the excitations have a dominant noncoherent particle-hole character. Several theoretical studies have been published recently dealing with the low-lying electric dipole strength in neutron-rich nuclei. For this low-lying electric dipole strength the notion ''pygmy dipole resonance'' (PDR) has been introduced. Here we use that name as the picture of an oscillation of a neutron skin against a core built of neutrons and protons for the PDR. The main conclusions of the models are presented here.

One requirement for the oscillation of the neutron skin against a core that produces the electric dipole strength in the hydrodynamical model is that such a skin indeed builds up. This is the case for the neutron-rich calcium isotopes as has been shown with the help of elastic proton scattering [58] in combination with electron scattering [59]. The data show that the proton rms-radii vary unsystematically between 3.38 and 3.42 fm while the extracted neutron rms-radii increase systematically from 3.42 fm for ^{40}Ca to 3.67 fm for ^{48}Ca. In conclusion the thickness of the neutron skin grows from about 0.03 fm for ^{40}Ca to 0.29 fm for ^{48}Ca. The results of an increasing difference in neutron and proton radii have recently been confirmed in experiments with antiprotonic atoms [60].

Speaking in terms of proton and neutron densities Im *et al.* have calculated the thickness of pure neutron matter in calcium isotopes from $A=40$ to $A=70$ within the Skyrme-Hartree-Fock model [61]. Their results show that while the matter density in the exterior region increases with mass number, the proton density in the exterior region decreases so that the matter density at the surface is more and more determined by the neutron density. In addition to the general trend of growing skin thickness it is argued that shell effects are not negligible ecspecially in the exterior region of the neutron density.

One explanation for the difference in the electric dipole strength of the two calcium isotopes is given within the phonon damping model (PDM). Here, the additional strength in ^{48}Ca is caused by noncollective particle-hole transitions which gain strength from the giant dipole resonance (GDR) phonon. The GDR is situated at almost the same energy of 19.0 MeV in both isotopes with widths of $\Gamma=5.0$ MeV for ^{40}Ca and $\Gamma=6.98$ MeV for ^{48}Ca [62,63]. Because of the different widths the influence on the low energy region may be different, too. Calculations within the phonon damping model (PDM) [64–67] agree quite well with our experimental data for ^{48}Ca. The PDM predicts an exhaustion of the EWSR of 0.52% [68], which overestimates our extracted value by 60%. For ^{40}Ca the results show an exhaustion of the EWSR of 0.2% [69] which is of the same order of magnitude as the calculation for ^{48}Ca, but one order of magnitude higher than our experimentally extracted value for ^{40}Ca. The significant experimental difference in the $E1$ strengths, is therefore not reproduced. It is important to note that the parameters of the PDM are adjusted to reproduce the gross structure of the GDR while investigations of γ-ray strength function models show that the extrapolation of the strength distribution down to energies below the particle threshold leads to unrealistic high dipole strengths and overestimates the experimental data [70–72]. Because of this fact there are attempts to describe experimental data of $E1$ strengths with modified Lorentzian functions introducing an energy dependent damping width or a low-energy $E_\gamma \rightarrow 0$ limit. There an additional Lorentzian function was added incoherently at lower energies to account for the PDR. Down to approximately 6 MeV the latter attempts seem to describe experimental data in higher mass nuclei quite well [73].

A more microscopic view is given within the relativistic random phase approximation (RRPA) to low-lying dipole strength in neutron rich oxygen and calcium isotopes [74]. Escpecially for calcium the calculations predict no dipole strength below 10 MeV for all isotopes with $A<54$, which is in contrast to our experimental findings. Analyzing the structure of the peaks in both the oxygen and the $A\geqslant 54$ calcium isotopes the authors conclude that all states are dominated by single-particle transitions which are almost exclusively caused by the neutrons in contrast to a coherent superposition of particle-hole configurations characterizing collective excitations.

Another approach to the low-lying electric dipole strength is given by Mohan *et al.* [22]. Their calculations within the three-fluid hydrodynamical model predict an excitation mode whose nature is very similar to that of the GDR but decoupled completely. This predicted excitation form should be observable in nuclei with a high neutron excess, i.e., high N/Z ratio. The model predicts a shift of the centroid energy down to lower energies with increasing mass and an increasing strength with increasing N/Z ratio. For the Ca isotopes, however, no quantitative prediction exists, and for the case of ^{208}Pb presented in Ref. [22] there is no quantitative agreement.

Calculations for the even-even calcium isotopes from ^{40}Ca to ^{48}Ca using the density functional theory were performed by Chambers *et al.* [24]. The calculations show additional broad resonances at low energies $E_x<10$ MeV in neutron-rich nuclei. Their nucleonic density variation is found to be an oscillation of the surface neutrons against the inert ^{40}Ca core. The calculations lead to energies of the PDR falling from approx. 9.1 MeV for ^{42}Ca to 7.6 MeV for ^{48}Ca with low-lying strength for ^{48}Ca of about 2% of the EWSR.

These examples show that the hydrodynamical models describe the behavior of the $E1$ strength distribution qualitatively, but differ among each other in the absolute values for the exhaustion of the EWSR. However, the microscopic approaches fail to describe the differences in the low-lying dipole strength distribution presented here.

D. Candidates for a $|2^+\otimes 3^-;1^-\rangle$ two phonon state

Up to now, the $|2^+\otimes 3^-;1^-\rangle$ two-phonon state is fairly well established in nuclei with $A\geqslant 100$ [3,7,11]. One question is whether this state can be observed in the medium mass nuclei ^{40,48}Ca at the $Z=20$ shell closure as well. It could be expected that with the decrease of collectivity of the vibrational phonons the collectivity of the multiphonon excitation ceases. From empirical systematics for nuclei with mass $A\geqslant 52$ it is possible to point out candidates for the $|2^+\otimes 3^-;1^-\rangle$ two-phonon states in the investigated nuclei. At first the excitation energy of the level should be close the

sum of the two single phonons, which is obvious in the harmonic picture. The second criterion arises from calculations of the strength of the two-phonon excitation. In a purely collective picture the coupling of the two single phonons should induce a dynamic dipole moment proportional to the dynamic quadrupole and octupole deformation parameters β_2 and β_3 [27, 75–77] via

$$D = -0.0065 \frac{e^2}{R_N} \frac{A}{C_1} Z \beta_2 \beta_3 e R_N \tag{4.4}$$

with R_N being the nuclear radius, C_1 the asymmetry energy of the Weizsäcker formula, and β_2 and β_3 symbolizing the quadrupole and octupole deformation parameters, respectively. These values are tabulated in the compliations of Raman [78] and Spears [79]. Although the properties discussed above are indicators of a possible two-phonon structure of a state, a proof can only be given by observing its decay pattern. The $B(E1)$ transition strength of the level is then proportional to the square of the dipole moment and the value $B(E1)/D^2$ is constant. We have to mention here that we used a newer parameter for the asymmetry energy [80] than [27] for our calculations of the dipole moments which causes a difference of about 25% in the results.

Turning to the calcium isotopes the situation is as follows: In ^{40}Ca the first 2_1^+ and 3_1^- states can be found at 3904 and 3737 keV, respectively. Therefore with harmonic coupling of the phonons the $|2^+ \otimes 3^-; 1^-\rangle$ state would be expected at an energy of 7641 keV. We find a 1^- state at 6950 keV. Since this state is the only one with considerable strength (as can be seen in Fig. 9) we suppose this one to be the candidate for the coupled $|2^+ \otimes 3^-; 1^-\rangle$ two-phonon state.

In ^{48}Ca the first excited states lie at energies of $E(2_1^+) = 3832$ keV and $E(3_1^-) = 4507$ keV so that the two-phonon state would be expected at an energy of 8339 keV. Our analysis shows two 1^- states that serve as candidates for the two phonon state, one at 7656 keV and another at 7299 keV. Since the $E1$ level-density is relatively high in this energy region, mixing between the states is very likely and a state of pure two-phonon character is not likely to persist.

For the strength-systematics we have the following situation: in ^{40}Ca the quadrupole and octupole deformation parameters of the first excited vibrational states are given by $\beta_2 = 0.122(10)$ and $\beta_3 = 0.433(36)$. From this the expected dipole moment of the coupled state is calculated to be with Eq. (4.4) to $0.023(4)e$ fm. From the empirical systematics taking an average value of $B(E1)/D^2 \approx 5$ [81] one would expect an induced electric dipole strength of about $2.5 \times 10^{-3}\, e^2\,\mathrm{fm}^2$. We find for the 1^- state at 6950 keV a strength of $B(E1)\uparrow = 4.2(6) \times 10^{-3}\, e^2\,\mathrm{fm}^2$.

For ^{48}Ca the harmonic coupling model predicts a dipole moment of $D = 0.012(5)e$ fm with the deformation parameters β_2 and β_3 given by 0.101(17) and 0.23(6), respectively. The same consideration as for ^{40}Ca leads to an expected electric dipole strength of the order of $0.7 \times 10^{-3}\, e^2\,\mathrm{fm}^2$.

The strengths of the candidates in ^{48}Ca are $B(E1)\uparrow = 1.4(1) \times 10^{-3}\, e^2\,\mathrm{fm}^2$ for the one at 7656 keV and $B(E1)\uparrow = 16.5(10) \times 10^{-3}\, e^2\,\mathrm{fm}^2$ for the one at 7299 keV.

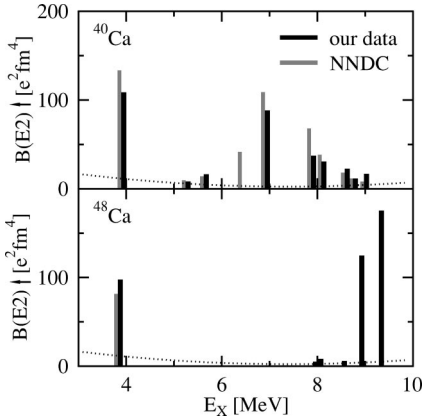

FIG. 10. Electric quadrupole strength distributions for ^{40}Ca (upper part) and ^{48}Ca (lower part). The strengths of ^{40}Ca are compared to NNDC data [44] which are mainly based on the results by Moreh *et al.* [53]. Only one disagreement can be seen in the $B(E2)$ distribution of ^{40}Ca, where a transition at 6421 keV has—according to our experimental findings—$E1$ character instead of the $E2$ character adopted from earlier measurements. The sum of the strengths below 10 MeV is of the same order of magnitude in both nuclei. The dotted line shows the sensitivity limit of the measurements on ^{40,48}Ca assuming $\Gamma_0 = \Gamma$.

This makes the former state the best candidate for a $2^+ \otimes 3^-$ structure. However, as has been pointed out above, mixing with the state at 7299 keV and other 1^- levels lying closely has to be taken into account. Detailed knowledge about the decay pattern are needed to give a definit conclusion [7].

E. E2 strength distributions

The measured $E2$ strength distribution is shown in Fig. 10. The results for ^{40}Ca agree nicely with previous data [44] as can be seen from the comparison of the black and gray bars in the figure. The excitation strength of the first 2_1^+ state in ^{48}Ca is also in agreement with literature, whereas the other $B(E2)$ values in this isotope have been measured for the first time.

The lower lines of Table IV contain the summed $E2$ strengths measured for the two Ca isotopes up to 9.9 MeV expressed in $e^2\,\mathrm{fm}^4$, in Weisskopf units (W.u.), and as percentage of the energy-weighted isoscalar $E2$ sum rule

$$S(E2) = \frac{25(\hbar c)^2 (Ze)^2}{4\pi A\, m_p c^2} \langle r^2 \rangle, \tag{4.5}$$

which amounts to about $10310\, e^2\,\mathrm{fm}^4$ MeV and $9366\, e^2\,\mathrm{fm}^4$ MeV for ^{40}Ca and ^{48}Ca, respectively [82]. The electric quadrupole strength below 10 MeV excitation energy amounts to $332(60)\, e^2\,\mathrm{fm}^4$ which corresponds to 8.2(15) W.u. for ^{40}Ca and to $407(32)\, e^2\,\mathrm{fm}^4$ corresponding to 7.9(6) W.u. in ^{48}Ca. While the summed strength in the two isotopes differs only on a small scale, the energy-weighted sum rules up to 10 MeV are exhausted to 20(3)% in ^{40}Ca as compared to 34(3)% in ^{48}Ca. The result for ^{40}Ca is in agreement with the results of Ref. [56] where 24(6)% of the $E2$-EWSR were

found, but the inelastic scattering observes considerably less for ^{48}Ca, namely, only 13(7)%.

The fact that the centroid of the $E2$ strength in ^{40}Ca is both lower and more fragmented than in ^{48}Ca indicates that the $N=28$ shell closure is more stringent than the double shell closure at $N=Z=20$. In addition, as has been noted for the $E1$ excitations, a fraction of the $E2$ strength in ^{40}Ca might escape detection due to proton emission above 8.4 MeV.

Continuum-RPA calculations of Kamerdzhiev *et al.* [83] have investigated the $E2$ strength distribution in the energy region of the isoscalar giant quadrupole resonance (IS-GDR) down to energies below the particle threshold. Due to ground-state correlations, i.e., mixing of the unperturbed IS-GQR states with complex configurations, the centroid of the IS-GQR is predicted at about 15 MeV, and a strong fragmentation of the strength is expected. Rough agreement with the predictions of Ref. [83] was found in recent studies using coincidence techniques following electron and hadron scattering [84]. For ^{40}Ca about 10 and 17 % of the EWSR have been detected between 11 and 15 MeV for the dominant p_0 and α_0 channels, respectively. The n_0 channel in scattering from ^{48}Ca carries about 10% of the EWSR between 11 and 14 MeV with further decay channels above 12 MeV which have not been taken into account.

Our present results, however, indicate that the EWSR is exhausted at low energies to a level comparable to the region around the predicted centroid of the IS-GQR, in conflict with theory. This should lead to a theoretical re-examination of the $E2$ strength distribution in medium-mass and light nuclei. The low-lying $E2$ strength might originate in an even lower centroid or stronger fragmentation of the IS-GQR, but it is also possible that the influence of isovector contributions at low excitation energies has been underestimated so far. The precision of our results demonstrates that photon scattering experiments are able to provide also valuable information towards understanding the electric giant quadrupole response in this mass region.

V. CONCLUSIONS AND OUTLOOK

In conclusion we have measured the dipole and electric quadrupole strength distributions of the two doubly magic nuclei ^{40}Ca and ^{48}Ca with the photon scattering method. We found candidates for the $|2^+\otimes 3^-;1^-\rangle$ two-phonon state in these two isotopes with the help of empirical systematics in the energy and ground state transition strength. While the summed $B(E2)$ strength below 10 MeV is almost equal in both isotopes, a considerable difference in the $B(E1)$ strength is found. Unfortunately—limited by our experimental setup and the particle emission thresholds of the investigated nuclei—we were only able to measure the strength distributions up to 10 MeV which is a somehow arbitrary energy limit.

None of the theoretical describtions was able to predict the main experimental findings about the $E1$ strength distributions in ^{40}Ca and ^{48}Ca, and the $E2$ strength observed experimentally is also unaccounted for by theory so far. This shows that even doubly magic stable nuclei may pose a challenge for model calculations. We hope that the presented new results can help to trigger refinements of the present nuclear structure models.

A systematic investigation of the nuclear structure of all stable even mass calcium isotopes will give more information on the nature of the excitations. NRF experiments on ^{42}Ca and ^{44}Ca are in preparation to see if the additional electric dipole strength increases with N/Z or if there is a connection between the GDR parameters and the observed dipole response. In addition results from $(p,p'\gamma)$ experiments will allow to observe the exact decay pattern of the states.

ACKNOWLEDGMENTS

We thank the S-DALINAC group around H.-D. Gräf for the support during the photon scattering experiments. We thank P. von Brentano, Y. Fujita, I. Hamamoto, F. Iachello, U. Kneissl, N. Pietralla, A. Richter, G. Schrieder, and K. Schweda for valuable discussions and the Gesellschaft für Schwerionenforschung (GSI) for the loan of the ^{48}Ca isotope material. This work was supported by the Deutsche Forschungsgemeinschaft (Contracts No. Zi 510/2-1 and FOR 272/2-2).

[1] F.R. Metzger, Prog. Nucl. Phys. **7**, 53 (1959).
[2] U. Kneissl, H.H. Pitz, and A. Zilges, Prog. Part. Nucl. Phys. **37**, 349 (1996).
[3] C. Fransen, O. Beck, P.v. Brentano, T. Eckert, R.D. Herzberg, U. Kneissl, H. Maser, A. Nord, N. Pietralla, H.H. Pitz, and A. Zilges, Phys. Rev. C **57**, 129 (1998).
[4] A. Zilges, P.v. Brentano, H. Friedrichs, R.D. Heil, U. Kneissl, S. Lindenstruth, H.H. Pitz, and C. Wesselborg, Z. Phys. A **340**, 155 (1991).
[5] A. Zilges, P.v. Brentano, R.D. Herzberg, U. Kneissl, J. Markgraf, and H.H. Pitz, Nucl. Phys. **A599**, 147c (1996).
[6] P.v. Brentano, A. Zilges, R.D. Heil, R.D. Herzberg, U. Kneissl, H.H. Pitz, and C. Wesselborg, Nucl. Phys. **A557**, 593c (1993).
[7] M. Wilhelm, E. Rademacher, A. Zilges, and P.v. Brentano, Phys. Rev. C **54**, R449 (1996).
[8] R.-D. Herzberg, P.v. Brentano, J. Eberth, J. Enders, R. Fischer, N. Huxel, T. Klemme, P.v. Neumann-Cosel, N. Nicolay, N. Pietralla, V.Yu. Ponomarev, J. Reif, A. Richter, C. Schlegel, R. Schwengner, S. Skoda, H.G. Thomas, I. Wiedenhöver, G. Winter, and A. Zilges, Phys. Lett. B **390**, 49 (1997).
[9] M. Wilhelm, S. Kasemann, G. Pascovici, E. Rademacher, P.v. Brentano, and A. Zilges, Phys. Rev. C **57**, 577 (1998).
[10] K. Govaert, F. Bauwens, J. Bryssinck, D. De Frenne, E. Jacobs, W. Mondelaers, L. Govor, and V.Yu. Ponomarev, Phys. Rev. C **57**, 2229 (1998).
[11] J. Bryssinck, L. Govor, D. Belic, F. Bauwens, O. Beck, P.v.

Brentano, D. De Frenne, T. Eckert, C. Fransen, K. Govaert, R.-D. Herzberg, E. Jacobs, U. Kneissl, H. Maser, A. Nord, N. Pietralla, H.H. Pitz, V.Yu. Ponomarev, and V. Werner, Phys. Rev. C **59**, 1930 (1999).

[12] J. Bryssinck, L. Govor, V.Yu. Ponomarev, F. Bauwens, O. Beck, D. Belic, P.v. Brentano, D. De Frenne, T. Eckert, C. Fransen, K. Govaert, R.-D. Herzberg., E. Jacobs, U. Kneissl, H. Maser, A. Nord, N. Pietralla, H.H. Pitz, and V. Werner, Phys. Rev. C **61**, 024309 (2000).

[13] F.R. Metzger, Phys. Rev. C **11**, 2085 (1975).

[14] K. Wienhard, C. Bläsing, K. Ackermann, K. Bangert, U.E.P. Berg, K. Kobras, W. Naatz, D. Rück, R.K.M. Schneider, and R. Stock, Z. Phys. A **302**, 185 (1981).

[15] W. Andrejtscheff, C. Kohstall, P. von Brentano, C. Fransen, U. Kneissl, N. Pietralla, and H.H. Pitz, Phys. Lett. B **506**, 239 (2001).

[16] A. Degener, C. Bläsing, R.D. Heil, A. Jung, U. Kneissl, H.H. Pitz, H. Schacht, S. Schennach, R. Stock, and C. Wesselborg, Nucl. Phys. **A513**, 29 (1990).

[17] J. Enders, P. von Brentano, J. Eberth, R.-D. Herzberg, N. Huxel, H. Lenske, P. von Neumann-Cosel, N. Nicolay, N. Pietralla, H. Prade, J. Reif, A. Richter, C. Schlegel, R. Schwengner, S. Skoda, H.G. Thomas, I. Wiedenhover, G. Winter, and A. Zilges, Nucl. Phys. **A636**, 139 (1998).

[18] F. Bauwens, J. Bryssinck, D. De Frenne, K. Govaert, L. Govor, M. Hagemann, J. Heyse, E. Jacobs, W. Mondelaers, and V.Yu. Ponomarev, Phys. Rev. C **62**, 024302 (2000).

[19] K. Ackermann, K. Bangert, U.E.P. Berg, G. Junghans, R.K.M. Schneider, R. Stock, and K. Wienhard, Nucl. Phys. **A372**, 1 (1981).

[20] U. E. P. Berg, Habilitation thesis, Giessen, 1985.

[21] P. Mohr, J. Enders, T. Hartmann, H. Kaiser, D. Schiesser, S. Schmitt, S. Volz, F. Wissel, and A. Zilges, Nucl. Instrum. Methods Phys. Res. A **423**, 480 (1999).

[22] R. Mohan, M. Danos, and L.C. Biedenharn, Phys. Rev. C **3**, 1740 (1971).

[23] Y. Suzuki, K. Ikeda, and H. Sato, Prog. Theor. Phys. **83**, 180 (1990).

[24] J. Chambers, E. Zaremba, J.P. Adams, and B. Castel, Phys. Rev. C **50**, R2671 (1994).

[25] J.P. Adams, B. Castel, and H. Sagawa, Phys. Rev. C **53**, 1016 (1996).

[26] S. Nakayama, T. Yamgata, H. Akimune, I. Daito, H. Fujimara, Y. Fujita, M. Fujiwara, K. Fushimi, T. Inomata, H. Kohri, N. Koori, K. Takahisa, A. Tamii, M. Tanaka, and H. Toyokawa, Phys. Rev. Lett. **85**, 262 (2000).

[27] F. Iachello, Phys. Lett. **160B**, 1 (1985).

[28] D.J. Millener, J.W. Olness, E.K. Warburton, and S.S. Hanna, Phys. Rev. C **28**, 497 (1983).

[29] J.W. Jury, B.L. Berman, D.D. Faul, P. Meyer, K.G. McNeill, and J.G. Woodsworth, Phys. Rev. C **19**, 1684 (1979).

[30] R. Anne, S.E. Arnell, R. Bimbot, H. Emling, D. Guillemaud-Mueller, P.G. Hansen, L. Johannsen, B. Jonson, M. Lewitowicz, S. Mattsson, A.C. Mueller, R. Neugart, G. Nyman, F. Pougheon, A. Richter, K. Riisager, M.G. Saint-Laurent, G. Schrieder, O. Sorlin, and K. Wilhelmsen, Phys. Lett. B **250**, 19 (1990).

[31] R.-D. Herzberg, C. Fransen, P.v. Brentano, J. Eberth, J. Enders, A. Fitzler L. Käubler, H. Kaiser, P.v. Neumann-Cosel, N. Pietralla, V.Yu. Ponomarev, H. Prade, A. Richter, H. Schnare, R. Schwengner, S. Skoda, H.G. Thomas, H. Tiesler, D. Weisshaar, and I. Wiedenhöver, Phys. Rev. C **60**, 051307 (1999).

[32] S. Volz, *et al.*, (unpublished).

[33] S. Volz, J. Enders, T. Hartmann, P. Mohr, K. Vogt, and A. Zilges, Balkan Phys. Lett. (to be published).

[34] J. Enders, P.v. Brentano, J. Eberth, A. Fitzler, C. Fransen, R.-D. Herzberg, H. Kaiser, L. Käubler, P.v. Neumann-Cosel, N. Pietralla, V.Yu. Ponomarev, H. Prade, A. Richter, H. Schnare, R. Schwengner, S. Skoda, H.G. Thomas, H. Tiesler, D. Weisshaar, and I. Wiedenhöver, Phys. Lett. B **486**, 279 (2000).

[35] H. Wickert, K. Ackermann, K. Bangert, U.E.P. Berg, C. Bläsing, W. Naatz, A. Ruckelshausen, S. Schennach, and R. Stock, Phys. Rev. C **34**, 835 (1986).

[36] R. Moreh, W.C. Sellyey, D.C. Sutton, and R. Vodhanel, Phys. Rev. C **37**, 2418 (1988).

[37] U. Kneissl, K.H. Leister, H.O. Neidel, and A. Weller, Nucl. Phys. **A272**, 125 (1976).

[38] J.G. Woodsworth, K.G. McNeill, J.W. Jury, R.A. Alvarez, B.L. Berman, D.D. Faul, and P. Meyer, Phys. Rev. C **19**, 1667 (1979).

[39] A. Leistenschneider, T. Aumann, K. Boretzky, D. Cortina, J. Cub, U. Datta Pramanik, W. Dostal, H. Emling, H. Geissel, A. Grünschloß, M. Hellström, R. Holzmann, S. Ilievski, N. Iwasa, M. Kaspar, A. Kleinböhl, J.V. Kratz, R. Kulessa, Y. Leifels, E. Lubkiewicz, G. Münzenberg, P. Reiter, M. Rejmund, C. Scheidenberger, C. Schlegel, H. Simon, J. Stroth, K. Sümmerer, E. Wajda, W. Walús, and S. Wan, Phys. Rev. Lett. **86**, 5442 (2001).

[40] E. Tryggestad, T. Aumann, D. Bazin, J.R. Beene, Y. Blumenfeld, M. Chartier, M.L. Halbert, P. Heckman, J.F. Liang, D.C. Radford, D. Shapira, B.M. Sherrill, M. Thoennessen, and R.L. Varner, Nucl. Phys. **A687**, 231c (2001).

[41] T. Hartmann, J. Enders, P. Mohr, K. Vogt, S. Volz, and A. Zilges, Phys. Rev. Lett. **85**, 274 (2000); **86**, 4981(E) (2001).

[42] Application Software Group, GEANT 3.21, CERN Program Library Long Writeup W5013, 1994.

[43] N. Pietralla, I. Bauske, O. Beck, P. von Brentano, W. Geiger, R.-D. Herzberg, U. Kneissl, J. Margraf, H. Maser, H.H. Pitz, and A. Zilges, Phys. Rev. C **51**, 1021 (1995).

[44] ENSDF data base, revision of 19-Aug-1999, using NNDC Online Data Service, based on Refs. [45–48] and updated with later experimental results.

[45] P.M. Endt and C.v.d. Leun, Nucl. Phys. **A310**, 1 (1978).

[46] P.M. Endt, Nucl. Phys. **A521**, 1 (1990); **A529**, 763(E) (1991); **A564**, 609(E) (1993).

[47] T.W. Burrows, Nucl. Data Sheets **68**, 1 (1993); $A=48$.

[48] F. Ajzenberg-Selove, Nucl. Phys. **A506**, 1 (1990).

[49] W. Steffen, H.-D. Gräf, W. Gross, D. Meuer, A. Richter, E. Spamer, O. Titze, and W. Knüpfer, Phys. Lett. B **95**, 23 (1980).

[50] K. Vogt, Diplomarbeit, Technische Universität Darmstadt, 2000.

[51] K. Vogt, P. Mohr, M. Babilon, J. Enders, T. Hartmann, C. Hutter, T. Rauscher, S. Volz, and A. Zilges, Phys. Rev. C **63**, 055802 (2001).

[52] J. Theuerkauf, S. Esser, S. Krink, M. Luig, N. Nicolay, and H. Wolters, Programm sc vs–view spectra (Version 6.65), Universität zu Köln, 1992 (unpublished).

[53] R. Moreh, W.M. Sandefuhr, W.C. Sellyey, D.C. Sutton, and R.

Vodhanel, Phys. Rev. C **25**, 1824 (1982).
[54] M. Babilon, Diploma thesis, TU-Darmstadt, 2001.
[55] A. Bohr, and B. R. Mottelson, *Nuclear Structure* (Benjamin, Reading, MA, 1975), Vol. II.
[56] S. Ottini-Hustache, N. Alamanos, F. Auger, B. Castel, Y. Blumenfeld, V. Chiste, N. Frascaria, A. Gillibert, C. Jouanne, V. Lapoux, F. Marie, M. Mittig, J.C. Roynette, and J.A. Scarpaci, Phys. Rev. C **59**, 3429 (1999).
[57] S.W. Kikstra, C. van der Leun, P.M. Endt, J.G.L. Booten, A.G.M. van Hees, and A.A. Wolters, Nucl. Phys. **A512**, 425 (1990).
[58] R.H. McCamis, T.N. Nasr, J. Birchall, N.E. Davison, R.F. Carlson, A.J. Cox, B.C. Clark, E.D. Cooper, S. Hama, and R.L. Mercer, Phys. Rev. C **33**, 1624 (1986).
[59] R.F. Frosch, R. Hofstadter, J.S. McCarthy, G.K. Noldeke, K.J. van Oostrum, M.R. Yearian, B.C. Clark, R. Herman, and D.G. Ravenhall, Phys. Rev. **174**, 1380 (1968).
[60] A. Trzcińska, J. Jastrębski, P. Lubiński, F.J. Hartmann, R. Schmidt, and T. von Egidy, Phys. Rev. Lett. **87**, 082501 (2001).
[61] S. Im and J. Meng, Phys. Rev. C **61**, 047302 (2000).
[62] A. Veyssiere, Nucl. Phys. **A227**, 513 (1974).
[63] G.J. O'Keefe, Nucl. Phys. **A469**, 239 (1987).
[64] N.D. Dang and A. Arima, Phys. Rev. Lett. **80**, 4145 (1998).
[65] N.D. Dang and A. Arima, Nucl. Phys. **A636**, 427 (1998).
[66] N.D. Dang, K. Tanabe, and A. Arima, Phys. Rev. C **58**, 3374 (1998).
[67] N.D. Dang, K. Tanabe, and A. Arima, Nucl. Phys. **A645**, 536 (1999).
[68] N.D. Dang, V.K. Au, T. Suzuki, and A. Arima, Phys. Rev. C **63**, 044302 (2001).
[69] N.D. Dang (private communication).
[70] D.F. Zaretskij and V.K. Sirotkin, Yad. Fiz. **27**, 1534 (1978) [Sov. J. Nucl. Phys. **27**, 1534 (1978)].
[71] S.G. Kadmesnskij, V.P. Markushew, and V.I. Furmann, Yad. Fiz. **37** 277, (1983) [Sov. J. Nucl. Phys. **37**, 227 (1983)].
[72] V.K. Sirotkin, Yad. Fiz. **43**, 570 (1986) [Sov. J. Nucl. Phys. **43**, 570 (1986)].
[73] J. Kopecky and M. Uhl, Phys. Rev. C **41**, 1941 (1990).
[74] D. Vretenar, N. Paar, P. Ring, and G. A. Lalazissis, Nucl. Phys. A (to be published).
[75] A. Bohr and B.R. Mottelson, Nucl. Phys. **4**, 529 (1957).
[76] A. Bohr and B.R. Mottelson, Nucl. Phys. **9**, 687 (1958).
[77] V. Strutinski, J. Nucl. Energy **4**, 523 (1957).
[78] S. Raman, C.H. Malarkey, W.T. Milner, C.W. Nestor, Jr., and P.H. Stelson, Phys. Rev. C **36**, 1 (1987).
[79] R.H. Spear, Phys. Rev. C **42**, 55 (1989).
[80] K. Vogt, T. Hartmann, and A. Zilges, Phys. Lett. B (to be published).
[81] M. Babilon (to be published).
[82] M. N. Harakeh, program BEL, as discussed in K. Schweda, Dissertation D17, Technische Universität Darmstadt, 2000.
[83] S. Kamerdzhiev, J. Speth, and G. Tertychny, Nucl. Phys. **A624**, 328 (1997).
[84] K. Schweda, J. Carter, A.A. Cowley, H. Diesener, R.W. Fearick, S.V. Förtsch, J.J. Lawrie, P. von Neumann-Cosel, J.V. Pilcher, A. Richter, F.D. Smit, G.F. Steyn, and S. Strauch, Phys. Lett. B **506**, 247 (2001).